STRUCTURAL CHEMISTRY

ISSN 2053-2296

Crystal structure of 3-deoxy-3-fluoro-α-D-galactopyranose monohydrate: structural comparisons to related monosaccharides

Wenhui Zhang,[a] Allen G. Oliver[b] and Anthony S. Serianni[b]*

[a]Omicron Biochemicals, Inc., 115 South Hill St., South Bend, IN 46617-2701, USA, and [b]Department of Chemistry & Biochemistry, University of Notre Dame, Notre Dame, IN 46556-5670, USA. *Correspondence e-mail: aseriann@nd.edu

Received 3 September 2026
Accepted 6 November 2026

Edited by I. D. Williams, Hong Kong University of Science and Technology, Hong Kong

Keywords: crystal structure; fluorosugar; fluorinated galactose; 3-fluoro-D-galactose; 3-deoxy-3-fluoro-D-galactose; 3-deoxy-3-fluoro-α-D-galactopyranose.

CCDC reference: 2601096

Supporting information: this article has supporting information at journals.iucr.org/c

3-Deoxy-3-fluoro-D-galactose, (I), was prepared chemically from 1,2;5,6-di-*O*-isopropylidene-α-D-gulofuranose, and after purification, was crystallized from water to give 3-deoxy-3-fluoro-α-D-galactopyranose, (II), as a monohydrate ($C_6H_{11}FO_5{\cdot}H_2O$). The structure of (II) was compared to those of several structurally-related unsubstituted and mono-fluorinated α-D-aldohexopyranoses. The aldohexopyranosyl ring in (II) adopts a $^4C_1$ chair form that is slightly skewed towards the $^3S_1$ conformer based on calculated Cremer–Pople puckering parameters. All the hydroxyl H atoms of (II) serve as hydrogen-bond donors, with three O atoms (O1, O4, and O6; standard galactopyranose numbering) serving as mono-acceptors and one O atom (O2) serving as a di-acceptor. The ring O atom is not hydrogen bonded in the crystal. The bound water molecule participates in four hydrogen bonds either with proximal saccharides or water. The F atom in (II) does not participate in hydrogen bonding, presumably because (II) contains sufficient hydroxyl O atoms to satisfy the hydrogen-bonding donor requirements of the hydroxyl H atoms. This behavior appears to be general, based on an inspection of the crystal structures of >10 mono-fluorinated compounds in the Cambridge Structural Database, with one exception (3-deoxy-3-fluoro-α-L-fucopyranose). The *gauche–trans* (*gt*) conformation is adopted by the exocyclic hydroxymethyl group in (II), and the anomeric hydroxyl H atom is roughly *trans* to C2, consistent with stereoelectronic factors that control C1—O1 bond rotation in (II).

1. Introduction

Fluorosugars are saccharide derivatives that have found diverse applications in carbohydrate chemistry and biochemistry, glycobiology, and enzymology. Replacement of the anomeric hydroxyl group with fluorine gives glycosyl fluorides that function as donors in chemical glycosylation (Yokoyama, 2000). Fluorosugars have been used in studies of enzyme reaction mechanisms by promoting stabilization of putative intermediates (White *et al.*, 1996). The hydrogen-bonding properties of saccharides are altered by fluorine substitution, which affects their binding properties to various receptors (Buchini *et al.*, 2008). For example, aldose reductase (E.C. 1.1.1.21) binds 3-deoxy-3-fluoro-D-galactose (3DFGal), (I) (Scheme 1), with an ∼10-fold higher affinity (K_m of 4.2 m*M*) than D-galactose, making this fluorinated sugar an attractive probe to investigate aldose reductase activity in the eye lens (Secchi *et al.*, 1999). 3DFGal, (I), has been shown to be a substrate for galactokinase (E.C. 2.7.1.6), with the resulting 3-deoxy-3-fluoro-α-D-galactopyranosyl 1-phosphate serving as a substrate for galactose-1-phosphate uridyl transferase (GALT) (E.C. 2.7.7.12) in the presence of UDP-glucose to give UDP-3DFGal (Thomas *et al.*, 1974; Barlow & Blanchard,

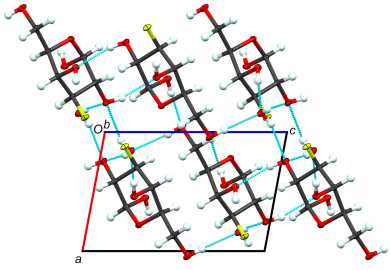

OPEN ACCESS
Published under a CC BY 4.0 licence

2000). UDP-3DFGal has been used in mechanistic studies of UDP-galactopyranose mutase (E.C. 5.4.99.9) that showed anomeric C—O bond cleavage occurs either *via* direct attack by a residue in the enzyme active site or *via* intramolecular attack of the axial O4 atom on the Gal anomeric C atom to give a bicyclic intermediate (Barlow & Blanchard, 2000). A library of mono-fluorinated Gal derivatives, including (I), has been created to screen lectins using ^{19}F NMR spectroscopy in order to chemically map hydroxyl groups of importance in carbohydrate–receptor recognition (Martínez *et al.*, 2020). In more recent work, mono- and difluorinated Gal residues have been incorporated enzymatically as terminal residues in complex-type *N*-glycans attached to the F_c fragment of IgG to enhance antibody-mediated effector functions, presumably caused by altered hydrogen bonding and other noncovalent interactions with protein receptors (Wang *et al.*, 2026). Chemical methods to prepare fluorinated D-galactoses have been reviewed recently (Zhang *et al.*, 2023).

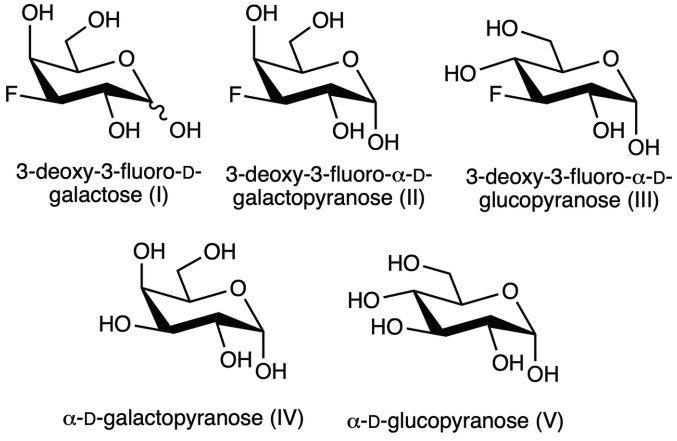

Scheme 1

Given the current resurgence of interest in fluorosugars as tools to control the biological functions of proteins and other macromolecules (Wang *et al.*, 2026), we report here the low-temperature X-ray structure of 3-deoxy-3-fluoro-α-D-galacto-pyranose (3DFαGal*p*), (II) (Scheme 1), crystallized from distilled water (Fig. 1). The unit cell contains two molecules each of saccharide and H_2O, with the water molecules each participating in four hydrogen bonds with four 3DFαGal molecules, twice as a donor with $O_{water}\cdots O_{saccharide}$ internuclear distances of ∼2.96 Å and twice as an acceptor with $O_{water}\cdots O_{saccharide}$ internuclear distances of ∼2.78 Å. The structural parameters in (II) are compared to those in the structurally-related 3-deoxy-3-fluoro-α-D-glucopyranose, (III) (Zhang *et al.*, 2010*b*), α-D-galactopyranose, (IV) (Kouwijzer *et al.*, 1995), and α-D-glucopyranose, (V) (Mostad *et al.*, 1994) (Scheme 1).

2. Experimental

2.1. Synthesis and crystallization

3-Deoxy-3-fluoro-D-galactose, (I), was synthesized by a chemical route described in the supporting information. The purified product was dissolved in a minimal volume of hot distilled water, and the solution was left at room temperature until clear colorless block-like crystals formed. Compound (I) crystallized as the α-pyranose monohydrate ($C_6H_{11}FO_5\cdot H_2O$), with two molecules of the saccharide and two molecules of water in the unit cell of the primitive noncentrosymmetric monoclinic space group $P2_1$.

Table 1
Experimental details.

Crystal data	
Chemical formula	$C_6H_{11}FO_5\cdot H_2O$
M_r	200.16
Crystal system, space group	Monoclinic, $P2_1$
Temperature (K)	120
a, b, c (Å)	5.8220 (3), 8.0494 (4), 8.7727 (5)
β (°)	100.6966 (12)
V (Å^3)	403.98 (4)
Z	2
Radiation type	Cu $K\alpha$
μ (mm^{-1})	1.42
Crystal size (mm)	0.18 × 0.15 × 0.10
Data collection	
Diffractometer	Bruker VENTURE
Absorption correction	Numerical (*SADABS*; Krause *et al.*, 2015)
T_{min}, T_{max}	0.776, 0.863
No. of measured, independent and observed [$I > 2\sigma(I)$] reflections	12551, 1632, 1628
R_{int}	0.030
(sin $\theta/\lambda)_{max}$ (Å^{-1})	0.625
Refinement	
$R[F^2 > 2\sigma(F^2)]$, $wR(F^2)$, S	0.022, 0.059, 1.10
No. of reflections	1632
No. of parameters	142
No. of restraints	1
H-atom treatment	H atoms treated by a mixture of independent and constrained refinement
$\Delta\rho_{max}$, $\Delta\rho_{min}$ (e Å^{-3})	0.24, −0.19
Absolute structure	Flack x determined using 745 quotients $[(I^+) - (I^-)]/[(I^+) + (I^-)]$ (Parsons *et al.*, 2013)
Absolute structure parameter	0.05 (3)

Computer programs: *APEX5* (Bruker, 2023), *SAINT* (Bruker, 2023), *SHELXT2018* (Sheldrick, 2015*a*), *SHELXL2025* (Sheldrick, 2015*b*), *Mercury* (Macrae *et al.*, 2020), *FinalCIF* (Kratzert, 2026), and *CIFTAB* (Sheldrick, 2008).

2.2. Refinement

Crystal data, data collection and structure refinement details are summarized in Table 1. Unless otherwise noted, H atoms were included in calculated positions, with C—H = 1.00 (methine) and 0.99 Å (methylene). Water and hydroxyl H atoms were refined freely. Atomic displacement parameters for the H atoms bonded to C atoms were tied to the equivalent isotropic displacement parameter of the atom to which they are bonded [U_{iso}(H) = 1.2U_{eq}(C)].

3. Results and discussion

Selected structural parameters in (II)–(V) are shown in Table 2. The endocyclic C—C bond lengths average 1.526 ± 0.007 Å, which is ∼0.01 Å longer than the average

Table 2
Comparison of structural parameters in (II)–(V).

Structural parameter	Compound			
	3DFαGal*p* (II)	3DFαGlc*p* (III)[a]	αGal*p* (IV)[b]	αGlc*p* (V)[c]
Bond lengths (Å)				
C1—C2	1.534 (2)	1.529 (2)	1.527 (4)	1.535 (2)
C2—C3	1.515 (2)	1.520 (2)	1.519 (4)	1.521 (2)
C3—C4	1.525 (2)	1.517 (2)	1.540 (4)	1.523 (2)
C4—C5	1.527 (2)	1.530 (2)	1.531 (4)	1.527 (2)
C5—C6	1.517 (2)	1.519 (2)	1.520 (4)	1.509 (2)
C1—O1	1.399 (2)	1.382 (2)	1.384 (3)	1.391 (3)
C1—O5	1.4181 (18)	1.4383 (19)	1.431 (3)	1.435 (2)
C2—O2	1.4286 (19)	1.4210 (19)	1.427 (4)	1.425 (2)
C3—O3			1.430 (4)	1.420 (2)
C3—F	1.4033 (18)	1.4029 (18)		
C4—O4	1.430 (2)	1.4265 (19)	1.429 (3)	1.431 (2)
C5—O5	1.4345 (19)	1.4358 (19)	1.436 (3)	1.434 (2)
C6—O6	1.429 (2)	1.434 (2)	1.424 (4)	1.425 (2)
Bond angles (°)				
C1—C2—C3	109.92 (13)	109.84 (13)	108.9 (2)	111.3 (1)
C2—C3—C4	112.41 (13)	111.89 (12)	109.5 (2)	109.7 (1)
C3—C4—C5	108.94 (13)	111.18 (12)	108.0 (2)	111.4 (1)
C4—C5—O5	111.11 (12)	109.13 (12)	111.0 (2)	108.5 (1)
C5—O5—C1	113.92 (12)	113.19 (11)	112.6 (2)	113.4 (1)
O5—C1—C2	109.60 (13)	108.39 (13)	108.6 (2)	110.0 (1)
C4—C5—C6	112.11 (13)	112.93 (13)	114.3 (2)	111.9 (1)
Torsion angles (°)				
C1—C2—C3—C4	−52.95 (17)	−52.12 (18)	−58.7 (3)	−51.25 (11)
C1—O5—C5—C4	61.07 (17)	62.59 (16)	61.4 (3)	62.34 (12)
C1—O5—C5—C6	−176.28 (12)	−174.52 (13)	−175.1 (2)	−176.13 (10)
C2—C3—C4—C5	51.74 (17)	50.26 (18)	55.9 (3)	53.56 (11)
C2—C1—O5—C5	−60.98 (17)	−64.88 (17)	−62.4 (3)	−60.91 (12)
C3—C4—C5—O5	−53.83 (16)	−53.49 (17)	−56.2 (3)	−57.89 (11)
C3—C2—C1—O5	55.51 (17)	57.49 (17)	60.5 (3)	54.19 (11)
C3—C4—C5—C6	−173.47 (13)	−173.10 (14)	−173.8 (2)	−177.00 (9)
C4—C5—C6—O6	−167.95 (13) (*gt*)[d]	57.27 (17) (*gg*)[d]	−62.6 (3) (*tg*)[d]	−170.13 (9) (*gt*)
O5—C5—C6—O6	70.02 (17) (*gt*)	−63.23 (17) (*gg*)	176.1 (2) (*tg*)	70.51 (12) (*gt*)
C2—C1—O1—H	–171.6 (18)	−177	−161 (3)	−156.8 (11)

Notes: (*a*) data obtained from the structure reported in Zhang *et al.* (2010*b*). (*b*) Data obtained from the structure reported in Kouwijzer *et al.* (1995). (*c*) Data obtained from the structure reported in Mostad *et al.* (1994). (*d*) *gg* is *gauche–gauche*, *gt* is *gauche–trans* and *tg* is *trans–gauche*.

exocyclic C5—C6 bond length in the four structures (1.516 ± 0.005 Å). The latter bond is expected to be shorter than the endocyclic bonds, but the extent of the difference will be influenced by hydroxyl C—O bond torsions (which affect C—C bond length) (Thibaudeau *et al.*, 2004), and on the torsional properties of the C5—C6 bond (*gg*/*gt*/*tg* conformations; *g* is *gauche* and *t* is *trans*) imposed by the crystalline lattice. In general, the C1—O1 bond lengths (1.389 ± 0.007 Å) are shorter than the C1—O5 and C5—O5 bond lengths (1.433 ± 0.006 Å), with the latter similar in length in each structure except for (II). Hydroxyl C—O bond lengths in (II)–(V) average 1.427 ± 0.004 Å, which is ∼0.03 Å longer than the C—F bond lengths (∼1.403 Å) [*e.g.* $r_{C3,O3}$ in (IV) is 1.43 Å, whereas $r_{C3,F}$ in (II) is 1.40 Å].

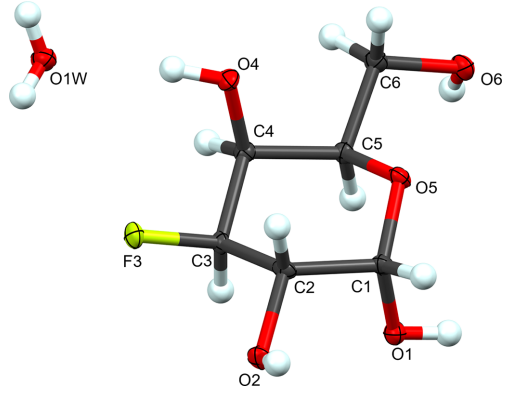

Figure 1
The structure of (II), showing the atom numbering. Displacement ellipsoids for the non-H atoms are depicted at the 50% probability level and H atoms are shown as small spheres of arbitrary radii. The water molecule participates in four hydrogen bonds with four proximal saccharides in the lattice.

Endocyclic C—C—C bond angles vary in the range 108.0 (2)–112.41 (13)°, giving an average of 110.2 ± 1.4°, and the average of the endocyclic C—C—O bond angles is comparable (109.5 ± 1.1°) (Table 2). Within the endocyclic C—C—C, C—C—O, and C—O—C bond angles, the latter are largest (113.3 ± 0.5°). The average of the exocyclic C4—C5—C6 bond angles is 112.8 ± 1.1°, comparable to that of the endocyclic C—O—C angles. The absolute values of the endocyclic C—C—C—C, C—O—C—C, and C—C—C—O torsion angles in (II)–(V) vary from 50.26 (18) to 62.59 (16)° (Table 2). The two angles that assume values near 60° asso-

Table 3
Cremer–Pople puckering parameters in (II)–(V).

Compound	Puckering parameter				
	θ (°)	ϕ (°)	Q (Å)	q_2 (Å)	q_3 (Å)
3DFαGal*p* (II)	2.61 (17)	21 (4)	0.5591 (17)	0.0257 (17)	0.5585 (17)
3DFαGlc*p* (III)[a]	6.35 (16)	26.0 (15)	0.5723 (16)	0.0638 (16)	0.5688 (16)
αGal*p* (IV)[b]	2.4 (3)	107 (6)	0.601 (3)	0.026 (3)	0.600 (3)
αGlc*p* (V)[c]	3.83 (13)	323.2 (19)	0.5696 (13)	0.0386 (13)	0.5684 (13)

Notes: (*a*) data obtained from the structure reported in Zhang *et al.* (2010*b*). (*b*) Data obtained from the structure reported in Kouwijzer *et al.* (1995). (*c*) Data obtained from the structure reported in Mostad *et al.* (1994).

ciated with idealized $^4C_1$ chair forms are C1—O5—C5—C4 and C2—C1—O5—C5. Thus, the C2—C1—O5—C5—C4 segment of the rings deviates least from the angles in the idealized $^4C_1$ chair forms, but the remaining four angles often deviate significantly from 60°, indicating distorted chair forms (see discussion of Cremer–Pople puckering parameters below). The C1—O5—C5—C6 torsion angles range from −174.52 (13) to −176.28 (12)°, and the C3—C4—C5—C6 angles range from −173.10 (14) to −177.00 (9)°, again indicating distortion from idealized $^4C_1$ chair forms. Exocyclic hydroxymethyl groups in (II) and (V) adopt the *gt* conformation, whereas in (III) and (IV), the *gg* and *tg* conformations are observed, respectively (Table 3). This behavior is consistent with solution NMR spectroscopy studies that show Glc rings prefer *gg* and *gt* conformations, whereas Gal rings prefer *gt* and *tg* conformations, based on semi-qualitative analyses of *J*-couplings (Thibaudeau *et al.*, 2004), and more recently on model-free *MA'AT* analyses (Meredith *et al.*, 2024). Although subject to greater uncertainty due to the low electron density of hydrogen, the C2—C1—O1—H torsion angles in (II)–(V) adopt values ranging from −156.8 (11) to −177°, which places the hydroxyl H atom in an orientation that optimizes the *exo*-anomeric effect (Thøgersen *et al.*, 1982; Kirby, 1983; Alabugin, 2016).

Cremer–Pople puckering parameters (Cremer & Pople, 1975) for the aldopyranosyl rings in (II)–(V) are summarized in Table 3. The extent of ring distortion, encoded in the value of θ, is smallest for (II) and (IV) (∼2.5°) and largest for (III) (6.4°). The direction of ring distortion, encoded in the value of ϕ, is similar for (II) and (III), with each distorted towards a $^3S_1$ conformer. Structure (IV) is distorted towards $^5S_1$ and structure (V) is distorted towards $^0S_2$. These ring distortions are minor and are revealed in the ring endocyclic torsion angles, which deviate significantly in some cases from idealized values of ±60° (see discussion above).

Hydrogen bonding in the crystalline lattices formed by (II)–(V) and by 4-deoxy-4-fluoro-β-D-glucopyranose, (VI), is summarized in Fig. 2. In all cases, all hydroxyl H atoms participate as donors to O atoms in proximal sugars or to water [the latter in (II) only]. In contrast, hydroxyl atoms O2–

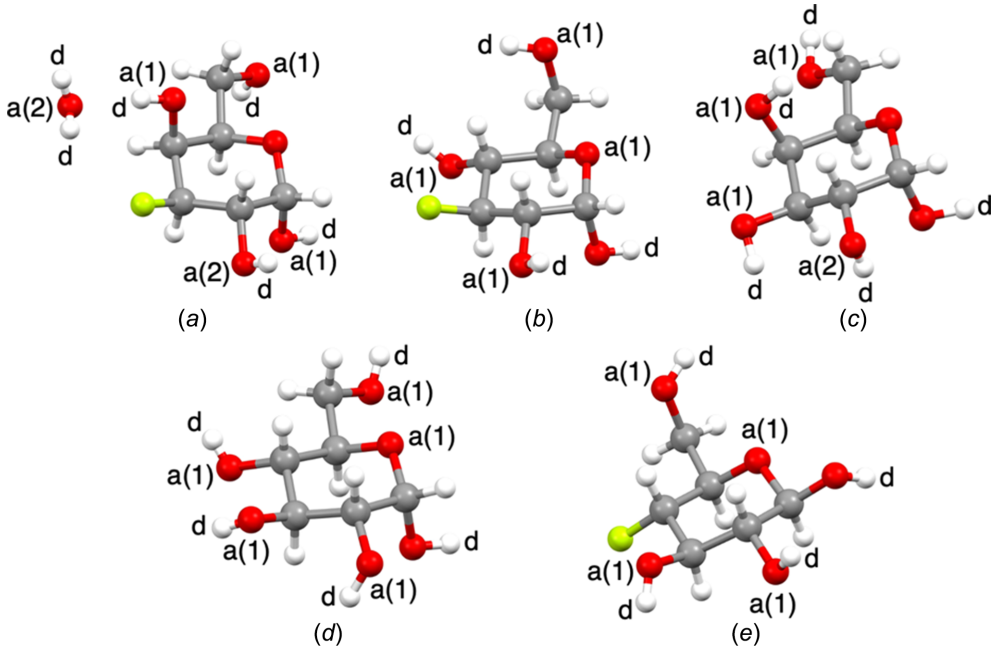

Figure 2
Hydrogen-bonding donors (d) and acceptors (a) in (*a*) (II), (*b*) (III), (*c*) (IV), (*d*) (V) and (*e*) 4-deoxy-4-fluoro-β-D-glucopyranose (VI) (Zhang *et al.*, 2010*a*). a(1) and a(2) denote O atoms participating as a mono-acceptor and di-acceptor, respectively. The F atoms in (II), (III), and (VI) do not serve as acceptors in the corresponding crystal structures.

Table 4
Hydrogen-bond geometry (Å, °).

D—H···A	D—H	H···A	D···A	D—H···A
O1—H1···O6^{i}	0.81 (3)	1.91 (3)	2.7202 (17)	174 (2)
O2—H2···O4^{ii}	0.80 (3)	1.96 (3)	2.7359 (17)	164 (3)
O4—H4···O1W	0.85 (3)	1.92 (3)	2.7644 (19)	172 (3)
O6—H6···O1W^{iii}	0.78 (3)	2.02 (3)	2.796 (2)	174 (3)
O1W—H1WA···O1^{iv}	0.77 (4)	2.55 (4)	2.978 (2)	117 (3)
O1W—H1WA···O2^{iv}	0.77 (4)	2.21 (4)	2.965 (2)	171 (4)
O1W—H1WB···F3^{v}	0.74 (4)	2.48 (4)	2.9355 (17)	122 (4)
O1W—H1WB···O2^{v}	0.74 (4)	2.25 (4)	2.9589 (19)	161 (4)

Symmetry codes: (i) $-x+2, y+\frac{1}{2}, -z+1$; (ii) $-x+1, y+\frac{1}{2}, -z$; (iii) $-x+1, y+\frac{1}{2}, -z+1$; (iv) $x, y-1, z$; (v) $-x, y-\frac{1}{2}, -z$.

O6 in (II)–(VI) are most commonly involved as mono-acceptors, and occasionally as di-acceptors [O2 of (II) and O2 of (IV)]. Within (II)–(VI), anomeric hydroxyl O atoms (O1) are less likely to serve as acceptors compared to O2–O6, with only (II) showing this behavior. Ring O atoms serve as mono-acceptors in (III), (V), and (VI), although statistically, ring O atoms in β-pyranoses [*e.g.* (VI)] are more likely to participate as acceptors than ring O atoms in α-pyranoses [*e.g.* (II)–(V)] due to delocalization of O5 lone-pair electrons into the C1—O5 bond in the latter [*endo*-anomeric effect (Lemieux, 1971; Kirby, 1983; Alabugin, 2016); reduced electron density on O5 in α-pyranoses]. In (II), (III), and (VI), the F atom does not participate as a hydrogen-bond acceptor [O1W···F = 2.9355 (12) Å and O—H···F = 122 (4)°, Table 4; average O···F = 2.85 (18) Å; the relatively tight O—H···F angle indicates a poor orientation for hydrogen bonding], an observation consistent with prior studies that show fluorine in small molecules does not serve as an acceptor if the molecule is rich in common acceptors such as oxygen or nitrogen. In the present case, (II)–(VI) have ample acceptors, thus disfavoring fluorine participation in hydrogen bonding (Taylor, 2017). The degree to which observations on hydrogen-bonding behavior in (II)–(VI) can be generalized remains to be determined through a comprehensive analysis of sugar and fluorosugar crystal structures available in the Cambridge Structural Database (Groom *et al.*, 2016), although an inspection of 12 additional mono- and di-fluorinated aldo- and ketopyranosyl rings found therein showed no evidence of fluorine serving as a hydrogen-bond acceptor, with one exception (Valverde *et al.*, 2020). In this structure (3-deoxy-3-fluoro-α-L-fucopyranose), bifurcated hydrogen bonds reduce the number of available hydroxyl O-atom acceptors in the lattice, apparently providing an opportunity for multiple F atoms to serve as secondary acceptors to proximal hydroxyl H atoms in a well-defined channel (Fig. S2 in the supporting information).

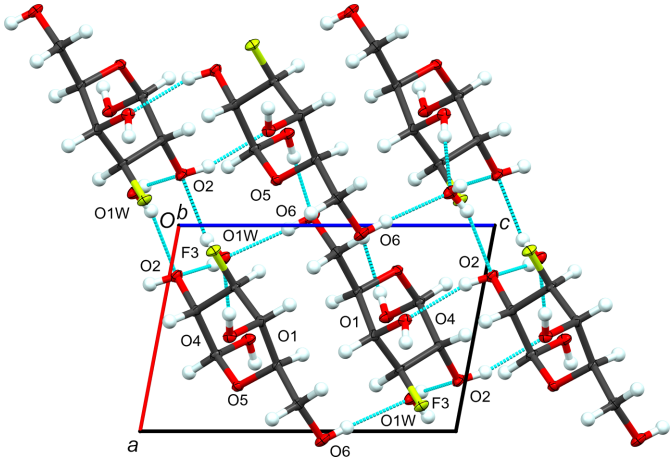

Figure 3
Packing diagram of (II), viewed along the b axis. Hydrogen bonds are shown as blue dashed lines.

The hydroxyl groups and water molecules form a three-dimensional hydrogen-bonded network within the crystal structure of (II) (Fig. 3). Hydroxyl atom O1 serves solely as a donor to hydroxyl atom O6^{i} on an adjacent molecule. Hydroxyl atom O2 is a donor to O4^{ii} and is a di-acceptor from two symmetry-related water molecules. Atom O4 is a mono-acceptor from O2 and is a donor in a hydrogen bond to the water of crystallization (O1W). Hydroxyl atom O6 is also a mono-acceptor, from O1, as noted, and is a donor to a water molecule (O6···O1W^{iii}). The water of crystallization is a di-acceptor (as noted from O4 and O6) and a di-donor to hydroxyl groups O2^{iv} and O2^{v}, related by translation and the screw axis along the b direction [symmetry codes: (i) $-x+2$, $y+\frac{1}{2}$, $-z+1$; (ii) $-x+1$, $y+\frac{1}{2}$, $-z$; (iii) $-x+1$, $y+\frac{1}{2}$, $-z+1$; (iv) x, $y-1$, z; (v) $-x$, $y-\frac{1}{2}$, $-z$; Table 4]. Two long contacts, that have a poor O—H···X geometry, are also noted. These are unlikely to be viable hydrogen-bond interactions (O1W···O1^{iv} and O1W···F3^{v}).

Funding information

The following funding is acknowledged: National Science Foundation, Directorate for Mathematical and Physical Sciences (award No. CHE-2241606 to Allen G. Oliver; award No. CHE-2002625 to Anthony S. Serianni).

References

Alabugin, I. V. (2016). In *Stereoelectronic Effects. A Bridge Between Structure and Reactivity*. Chichester: John Wiley & Sons.
Barlow, J. N. & Blanchard, J. S. (2000). *Carbohydr. Res.* **328**, 473–480.
Bruker (2023). *APEX5* and *SAINT*. Bruker AXS Inc., Madison, Wisconsin, USA.
Buchini, S., Buschiazzo, A. & Withers, S. G. (2008). *Angew. Chem. Int. Ed.* **47**, 2700–2703.
Cremer, D. & Pople, J. A. (1975). *J. Am. Chem. Soc.* **97**, 1354–1358.
Groom, C. R., Bruno, I. J., Lightfoot, M. P. & Ward, S. C. (2016). *Acta Cryst.* B**72**, 171–179.
Kirby, A. J. (1983). In *The Anomeric Effect and Related Stereoelectronic Effects at Oxygen*. Berlin: Springer Verlag.
Kouwijzer, M. L. C. E., van Eijck, B. P., Kooijman, H. & Kroon, J. (1995). *Acta Cryst.* B**51**, 209–220.
Kratzert, D. (2026). *FinalCif*. https://dkratzert.de/finalcif.html.
Krause, L., Herbst-Irmer, R., Sheldrick, G. M. & Stalke, D. (2015). *J. Appl. Cryst.* **48**, 3–10.
Lemieux, R. U. (1971). *Pure Appl. Chem.* **25**, 527–548.
Macrae, C. F., Sovago, I., Cottrell, S. J., Galek, P. T. A., McCabe, P., Pidcock, E., Platings, M., Shields, G. P., Stevens, J. S., Towler, M. & Wood, P. A. (2020). *J. Appl. Cryst.* **53**, 226–235.
Martínez, J. D., Manzano, A. I., Calviño, E., Diego, A., Rodriguez de Francisco, B., Romanò, C., Oscarson, S., Millet, O., Gabius, H.-J.,

Jiménez-Barbero, J. & Cañada, F. J. (2020). *J. Org. Chem.* **85**, 16072–16081.
Meredith, R. J., Yoon, M.-K., Carmichael, I. & Serianni, A. S. (2024). *J. Phys. Chem. B* **128**, 2360–2370.
Mostad, A., Neumann, K., Larsen, S., Wang, D., Springborg, J., Paulsen, G. B., Nielsen, R. I., Olsen, C. E., Pedersen, C. & Stidsen, C. E. (1994). *Acta Chem. Scand.* **48**, 276–278.
Parsons, S., Flack, H. D. & Wagner, T. (2013). *Acta Cryst.* B**69**, 249–259.
Secchi, E. F., Lizak, M. J., Sato, S. & Kador, P. F. (1999). *Curr. Eye Res.* **18**, 277–282.
Sheldrick, G. M. (2008). *Acta Cryst.* A**64**, 112–122.
Sheldrick, G. M. (2015*a*). *Acta Cryst.* A**71**, 3–8.
Sheldrick, G. M. (2015*b*). *Acta Cryst.* C**71**, 3–8.
Taylor, R. (2017). *Acta Cryst.* B**73**, 474–488.
Thibaudeau, C., Stenutz, R., Hertz, B., Klepach, T., Zhao, S., Wu, Q., Carmichael, I. & Serianni, A. S. (2004). *J. Am. Chem. Soc.* **126**, 15668–15685.
Thøgersen, H., Lemieux, R. U., Bock, K. & Meyer, B. (1982). *Can. J. Chem.* **60**, 44–57.
Thomas, P., Bessell, E. M. & Westwood, J. H. (1974). *Biochem. J.* **139**, 661–664.
Valverde, P., Vendeville, J.-B., Hollingsworth, K., Mattey, A. P., Keenan, T., Chidwick, H., Ledru, H., Huonnic, K., Huang, K., Light, M. E., Turner, N., Jiménez-Barbero, J., Galan, M. C., Fascione, M. A., Flitsch, S., Turnbull, W. B. & Linclau, B. (2020). *Chem. Commun.* **56**, 6408–6411.
Wang, X., Gomozkova, M., Li, S., Banerjee, B., Zong, G., Missiakas, D. & Wang, L.-X. (2026). *Proc. Nat. Acad. Sci. USA* **123**, e2530653123.
White, A., Tull, D., Johns, K., Withers, S. G. & Rose, D. R. (1996). *Nat. Struct. Mol. Biol.* **3**, 149–154.
Yokoyama, M. (2000). *Carbohydr. Res.* **327**, 5–14.
Zhang, H., Mei, H., Li, M., Liu, Z., Han, J. & Cao, Y. (2023). *Ind. Crops Prod.* **197**, 116671.
Zhang, W., Oliver, A. G. & Serianni, A. S. (2010*a*). *Acta Cryst.* C**66**, o496–o498.
Zhang, W., Oliver, A. G. & Serianni, A. S. (2010*b*). *Acta Cryst.* C**66**, o557–o560.

supporting information

Acta Cryst. (2026). C**82**, 811-816 [https://doi.org/10.1107/S2053229626011605]

Crystal structure of 3-deoxy-3-fluoro-α-D-galactopyranose monohydrate: structural comparisons to related monosaccharides

Wenhui Zhang, Allen G. Oliver and Anthony S. Serianni

Computing details

(I)

Crystal data

$C_6H_{11}FO_5 \cdot H_2O$
$M_r = 200.16$
Monoclinic, $P2_1$
$a = 5.8220$ (3) Å
$b = 8.0494$ (4) Å
$c = 8.7727$ (5) Å
$\beta = 100.6966$ (12)°
$V = 403.98$ (4) Å^3
$Z = 2$
$F(000) = 212$
$D_x = 1.646$ Mg m^{-3}
Cu $K\alpha$ radiation, $\lambda = 1.54178$ Å
Cell parameters from 9918 reflections
$\theta = 5.1$–74.5°
$\mu = 1.42$ mm^{-1}
$T = 120$ K
Block, colourless
0.18 × 0.15 × 0.10 mm

Data collection

Bruker VENTURE diffractometer
Radiation source: micro-focus, Incoatec Diamond
HELIOS Multi-layer monochromator
Detector resolution: 7.41 pixels mm^{-1}
combination of ω and φ–scans
Absorption correction: numerical (SADABS; Krause *et al.*, 2015)
$T_{min} = 0.776$, $T_{max} = 0.863$
12551 measured reflections
1632 independent reflections
1628 reflections with $I > 2\sigma(I)$
$R_{int} = 0.030$
$\theta_{max} = 74.6°$, $\theta_{min} = 5.1°$
$h = -7 \rightarrow 7$
$k = -10 \rightarrow 10$
$l = -10 \rightarrow 10$

Refinement

Refinement on F^2
Least-squares matrix: full
$R[F^2 > 2\sigma(F^2)] = 0.022$
$wR(F^2) = 0.059$
$S = 1.10$
1632 reflections
142 parameters
1 restraint
Primary atom site location: dual
Secondary atom site location: difference Fourier map
Hydrogen site location: mixed
H atoms treated by a mixture of independent and constrained refinement
$w = 1/[\sigma^2(F_o^2) + (0.0314P)^2 + 0.0961P]$ where $P = (F_o^2 + 2F_c^2)/3$
$(\Delta/\sigma)_{max} < 0.001$
$\Delta\rho_{max} = 0.24$ e Å^{-3}
$\Delta\rho_{min} = -0.19$ e Å^{-3}
Absolute structure: Flack *x* determined using 745 quotients [(I+)-(I-)]/[(I+)+(I-)] (Parsons *et al.*, 2013)
Absolute structure parameter: 0.05 (3)

Special details

Geometry. All esds (except the esd in the dihedral angle between two l.s. planes) are estimated using the full covariance matrix. The cell esds are taken into account individually in the estimation of esds in distances, angles and torsion angles; correlations between esds in cell parameters are only used when they are defined by crystal symmetry. An approximate (isotropic) treatment of cell esds is used for estimating esds involving l.s. planes.

Refinement. An arbitrary sphere of data was collected on a crystal having approximate dimensions of 0.176 × 0.147 × 0.101 mm, on a Bruker Venture diffractometer equipped with a Bruker PHOTON III detector using a combination of ω- and φ-scans of 0.5° (Bruker, 2023). Data were corrected for absorption and polarization effects and analyzed for space group determination (Krause *et al.*, 2015). The structure was solved by dual-space methods and expanded routinely (Sheldrick, 2015*a*). The model was refined by full-matrix least-squares analysis of F^2 against all reflections (Sheldrick, 2015*b*, Table 1). All non-H atoms were refined with anisotropic atomic displacement parameters.

Fractional atomic coordinates and isotropic or equivalent isotropic displacement parameters (Å²)

	x	*y*	*z*	U_{iso}*/U_{eq}
F3	0.12270 (17)	0.47600 (12)	0.12406 (12)	0.0144 (2)
O1	0.5540 (2)	0.88606 (15)	0.28768 (14)	0.0141 (3)
H1	0.670 (4)	0.939 (3)	0.323 (3)	0.018 (6)*
O2	0.2465 (2)	0.78687 (15)	0.02295 (14)	0.0133 (3)
H2	0.286 (4)	0.809 (4)	−0.057 (3)	0.025 (6)*
O4	0.5397 (2)	0.32513 (15)	0.22747 (14)	0.0127 (3)
H4	0.431 (5)	0.254 (4)	0.212 (3)	0.033 (7)*
O5	0.7817 (2)	0.64606 (14)	0.28306 (13)	0.0117 (3)
O6	1.0423 (2)	0.54207 (16)	0.58287 (15)	0.0160 (3)
H6	0.982 (5)	0.568 (4)	0.652 (3)	0.027 (7)*
C1	0.6299 (3)	0.7634 (2)	0.19550 (19)	0.0116 (3)
H1A	0.714925	0.818383	0.120112	0.014*
C2	0.4152 (3)	0.6738 (2)	0.10411 (19)	0.0112 (3)
H2A	0.466882	0.596757	0.027590	0.013*
C3	0.2970 (3)	0.5736 (2)	0.21372 (18)	0.0102 (3)
H3A	0.224013	0.650683	0.280403	0.012*
C4	0.4660 (3)	0.4573 (2)	0.31621 (19)	0.0104 (3)
H4A	0.386310	0.409068	0.397638	0.013*
C5	0.6785 (3)	0.5569 (2)	0.39492 (18)	0.0103 (3)
H5A	0.627724	0.638310	0.468174	0.012*
C6	0.8678 (3)	0.4465 (2)	0.4847 (2)	0.0132 (4)
H6A	0.796552	0.367164	0.548570	0.016*
H6B	0.941663	0.381635	0.410862	0.016*
O1W	0.1612 (2)	0.11283 (19)	0.15976 (16)	0.0162 (3)
H1WA	0.191 (7)	0.026 (6)	0.133 (4)	0.056 (11)*
H1WB	0.070 (7)	0.148 (6)	0.097 (5)	0.066 (13)*

Atomic displacement parameters (Å²)

	U^{11}	U^{22}	U^{33}	U^{12}	U^{13}	U^{23}
F3	0.0112 (5)	0.0145 (5)	0.0153 (5)	−0.0030 (4)	−0.0028 (4)	−0.0016 (4)
O1	0.0119 (6)	0.0129 (6)	0.0163 (6)	−0.0003 (5)	−0.0005 (5)	−0.0021 (5)
O2	0.0123 (5)	0.0154 (6)	0.0110 (6)	0.0015 (5)	−0.0011 (4)	0.0035 (5)
O4	0.0123 (6)	0.0104 (6)	0.0150 (6)	−0.0007 (5)	0.0018 (4)	−0.0040 (4)

O5	0.0085 (5)	0.0141 (6)	0.0120 (5)	0.0018 (4)	0.0007 (4)	0.0033 (5)
O6	0.0138 (6)	0.0166 (6)	0.0147 (6)	0.0005 (5)	−0.0049 (5)	−0.0007 (5)
C1	0.0102 (7)	0.0118 (8)	0.0121 (7)	0.0012 (6)	0.0004 (6)	0.0028 (6)
C2	0.0108 (8)	0.0125 (8)	0.0095 (7)	0.0021 (6)	−0.0005 (6)	0.0010 (6)
C3	0.0084 (7)	0.0116 (8)	0.0096 (7)	−0.0014 (6)	−0.0008 (6)	−0.0022 (6)
C4	0.0108 (7)	0.0110 (8)	0.0095 (7)	0.0002 (6)	0.0018 (6)	−0.0010 (6)
C5	0.0104 (8)	0.0115 (7)	0.0082 (7)	−0.0003 (6)	−0.0001 (6)	0.0009 (6)
C6	0.0133 (8)	0.0118 (8)	0.0131 (8)	0.0006 (6)	−0.0014 (6)	0.0006 (6)
O1W	0.0161 (6)	0.0128 (6)	0.0174 (7)	0.0009 (5)	−0.0025 (5)	0.0000 (5)

Geometric parameters (Å, º)

F3—C3	1.4033 (18)	C2—C3	1.515 (2)
O1—C1	1.399 (2)	C2—H2A	1.0000
O1—H1	0.81 (3)	C3—C4	1.525 (2)
O2—C2	1.4286 (19)	C3—H3A	1.0000
O2—H2	0.80 (3)	C4—C5	1.527 (2)
O4—C4	1.430 (2)	C4—H4A	1.0000
O4—H4	0.85 (3)	C5—C6	1.517 (2)
O5—C1	1.4181 (18)	C5—H5A	1.0000
O5—C5	1.4345 (19)	C6—H6A	0.9900
O6—C6	1.429 (2)	C6—H6B	0.9900
O6—H6	0.78 (3)	O1W—H1WA	0.77 (4)
C1—C2	1.534 (2)	O1W—H1WB	0.74 (4)
C1—H1A	1.0000		
C1—O1—H1	105.4 (17)	C2—C3—H3A	109.5
C2—O2—H2	107.1 (19)	C4—C3—H3A	109.5
C4—O4—H4	107.5 (19)	O4—C4—C3	111.20 (13)
C1—O5—C5	113.92 (12)	O4—C4—C5	109.71 (12)
C6—O6—H6	104 (2)	C3—C4—C5	108.94 (13)
O1—C1—O5	112.89 (13)	O4—C4—H4A	109.0
O1—C1—C2	108.67 (12)	C3—C4—H4A	109.0
O5—C1—C2	109.60 (13)	C5—C4—H4A	109.0
O1—C1—H1A	108.5	O5—C5—C6	106.97 (13)
O5—C1—H1A	108.5	O5—C5—C4	111.11 (12)
C2—C1—H1A	108.5	C6—C5—C4	112.11 (13)
O2—C2—C3	107.71 (13)	O5—C5—H5A	108.9
O2—C2—C1	112.26 (13)	C6—C5—H5A	108.9
C3—C2—C1	109.92 (13)	C4—C5—H5A	108.9
O2—C2—H2A	109.0	O6—C6—C5	111.35 (13)
C3—C2—H2A	109.0	O6—C6—H6A	109.4
C1—C2—H2A	109.0	C5—C6—H6A	109.4
F3—C3—C2	107.98 (12)	O6—C6—H6B	109.4
F3—C3—C4	107.90 (13)	C5—C6—H6B	109.4
C2—C3—C4	112.41 (13)	H6A—C6—H6B	108.0
F3—C3—H3A	109.5	H1WA—O1W—H1WB	107 (4)

C5—O5—C1—O1	60.29 (17)	C2—C3—C4—O4	−69.29 (17)
C5—O5—C1—C2	−60.98 (17)	F3—C3—C4—C5	170.70 (12)
O1—C1—C2—O2	51.59 (17)	C2—C3—C4—C5	51.74 (17)
O5—C1—C2—O2	175.37 (12)	C1—O5—C5—C6	−176.28 (12)
O1—C1—C2—C3	−68.27 (16)	C1—O5—C5—C4	61.07 (17)
O5—C1—C2—C3	55.51 (17)	O4—C4—C5—O5	68.11 (16)
O2—C2—C3—F3	65.54 (15)	C3—C4—C5—O5	−53.83 (16)
C1—C2—C3—F3	−171.87 (12)	O4—C4—C5—C6	−51.53 (17)
O2—C2—C3—C4	−175.54 (12)	C3—C4—C5—C6	−173.47 (13)
C1—C2—C3—C4	−52.95 (17)	O5—C5—C6—O6	70.02 (17)
F3—C3—C4—O4	49.67 (16)	C4—C5—C6—O6	−167.95 (13)

Hydrogen-bond geometry (Å, º)

D—H···*A*	*D*—H	H···*A*	*D*···*A*	*D*—H···*A*
O1—H1···O6^{i}	0.81 (3)	1.91 (3)	2.7202 (17)	174 (2)
O2—H2···O4^{ii}	0.80 (3)	1.96 (3)	2.7359 (17)	164 (3)
O4—H4···O1*W*	0.85 (3)	1.92 (3)	2.7644 (19)	172 (3)
O6—H6···O1*W*^{iii}	0.78 (3)	2.02 (3)	2.796 (2)	174 (3)
O1*W*—H1*WA*···O1^{iv}	0.77 (4)	2.55 (4)	2.978 (2)	117 (3)
O1*W*—H1*WA*···O2^{iv}	0.77 (4)	2.21 (4)	2.965 (2)	171 (4)
O1*W*—H1*WB*···F3^{v}	0.74 (4)	2.48 (4)	2.9355 (17)	122 (4)
O1*W*—H1*WB*···O2^{v}	0.74 (4)	2.25 (4)	2.9589 (19)	161 (4)

Symmetry codes: (i) −*x*+2, *y*+1/2, −*z*+1; (ii) −*x*+1, *y*+1/2, −*z*; (iii) −*x*+1, *y*+1/2, −*z*+1; (iv) *x*, *y*−1, *z*; (v) −*x*, *y*−1/2, −*z*.